Optica Applicata, Vol. XXXIII, No. 4, 2003

Raman gain characterization in standard single mode optical fibres for optical simulation purposes

PAULO S. ANDRÉ[1, 2], ROSÁRIO CORREIA[2], LUÍS M. BORGHESI JR[3], ANTÓNIO L.J. TEIXEIRA[1, 4], ROGÉRIO N. NOGUEIRA[1, 2], MÁRIO J.N. LIMA[1, 4], HYPOLITO J. KALINOWSKI[3], FERREIRA DA ROCHA[1, 4], JOÃO L. PINTO[1, 2]

[1]Instituto de Telecomunicações – Pólo de Aveiro, 3810-193 Aveiro, Portugal, e-mail: pandre@av.it.pt.

[2]Departamento de Física da Universidade de Aveiro, 3810-193 Aveiro, Portugal.

[3]Centro Federal de Educação Tecnológica do Paraná, Av. Sete de Setembro, 3165 80230-901 Curitiba, Brazil.

[4]Departamento de Electrónica e Telecomunicações da Universidade de Aveiro, 3810-193 Aveiro, Portugal.

We report on the measurement of the Raman gain coefficient in a standard single mode optical fibre (SMF), based on the power transfer between a high intensity pump signal and a counter-propagated broadband probe signal technique. The results were complemented with spontaneous Raman spectroscopy. The values of 7.48×10^{-27} $mW^{-1}Hz^{-1}$, 0.540×10^{-13} mW^{-1}, 3.03 fs, 12.40 fs, 40.78 fs and 0.160 were experimentally obtained for the Raman gain slope, maximum value of the gain coefficient, Raman time constant, first and second parameters of the Raman response function and fractional contribution of the delayed Raman response, respectively.

Keywords: simulated Raman scattering, optical fibre, optical communications.

1. Introduction

In a non-linear medium the quasi-monochromatic scattered light will consist mainly of light of the same frequency as the incident one. There may also be observed low intensity signals partially scattered, being up- and downshifted in frequency with respect to the incident light. These optical beams with a frequency up- and downshifted by an amount determined by the molecular vibration frequency modes of the medium are due to inelastic scattering by the irradiated substance. This phenomenon predicted in 1923 by Adolf Sneckal and observed years latter by Sir Chandresekhara Vankata Raman is known as spontaneous Raman scattering [1]. In terms of quantum mechanics the Raman effect is described as a non-linear parametric interaction between light and

molecular vibrations or the scattering of an incident photon by the medium to a higher or lower frequency photon, while at the same time the medium makes a transition between two vibrational states. The Raman effect can be understood as the annihilation of a pump photon creating a Stokes photon and an optical phonon simultaneously. When the scattered photon has a higher frequency than the incident one, it is called anti-Stokes photon. Since this process depends on the existence of optical phonons, therefore it is temperature dependent and much less intense at room temperature.

In a crystalline material the Stokes waves have specific and well defined frequencies. Due to the non-crystalline nature of the silica glasses, the Stokes wave frequency in optical fibres extends continuously over a broadband.

For a very intense pump wave (higher than a threshold value) the Stokes wave grows rapidly inside the medium and most of the pump energy is transferred to it. This phenomenon is known as stimulated Raman scattering (SRS).

The stimulated Raman scattering is one of the dominant fibre non-linear effects, which limits the allowed fibre input power in many optical communication systems, limiting the transmission of high intensity optical signals, for example, for remote optical pumping [2]. In dense wavelength division multiplexed (DWDM) systems, the SRS is also responsible for the power transference from lower wavelength channels to higher wavelength channels [3], causing a gain tilt in the power of channels [4], [5], and crosstalk between them [6], [7]. SRS also affects the systems of single channel optical solitons, since the Raman self-frequency shift effect induces a continuous downshift of the centre frequency of its spectrum [8].

In order to calculate, understand and deal with constrains imposed by the Raman effect it is necessary to know precisely the Raman gain coefficient and its distribution along the wavelength working interval.

We characterize the SRS in an optical fibre and obtain the necessary parameters to solve the propagation equation that describes the evolution of an optical pulse in the fibre. For characterization purposes, use is made of a continuous wave pump method, complemented with spontaneous Raman scattering measurements.

The present paper is divided into the following parts. In Section 2, we describe the simulation of an optical pulse in an optical fibre. Section 3 presents the analysis of the SRS. Section 4 shows the experimental method used to assess the simulation parameter. This assessment is complemented with measurements of spontaneous Raman scattering in Section 5. In Section 6, the experimental results are compared with the simulation ones. Finally, in Section 7, we outdraw some conclusions.

2. Simulation of wave propagation in optical fibres

The basic propagation equation of an optical pulse in an optical fibre (NLSE – non-linear Schrödinger equation) is a non-linear partial differential equation that does not generally leads to analytical solutions. Therefore, it is necessary to use numerical methods to solve it, with the split-step Fourier (beam propagation) being more intensively used. In this procedure, the propagation equation is split into two terms:

i) one is a linear differential operator that accounts for the dispersion and the absorption, ii) the other is a non-linear operator that governs the effects of fibre non-linearities. If we assume propagation over small step distance, the dispersive and non-linear effects can be considered to act independently. So, the simulation is carried out in two steps, in the first, the non-linearities act alone, in the second, the dispersion and attenuation act along. The simulation for the non-linear operator is carried out in the temporal domain and the simulation of the linear operator is performed in the frequency domain.

The most common form of the NLSE, which describes the pulse envelope amplitude A, during propagation over a distance z and over time t, is the following [9]:

$$\frac{dA}{dz} = -\beta_1 \frac{dA}{dt} - \frac{j}{2}\beta_2 \frac{d^2A}{dt^2} + \frac{1}{6}\beta_3 \frac{d^3A}{dt^3} - \frac{\alpha}{2}A + j\gamma|A|^2A - \frac{\gamma}{\omega_0}\frac{d(|A|^2A)}{dt} - j\gamma T_R A \frac{d|A|^2}{dt} \tag{1}$$

where α is the attenuation, β_1 stands for the inverse of the group velocity, β_2 is the group velocity dispersion, β_3 – third order group velocity dispersion, γ – non-linear coefficient, ω_0 represents the carrier frequency and T_R is the Raman time constant.

This form for the NLSE is approximated, and for simulation of optical pulses shorter than 100 fs, it should be changed to [10]

$$\frac{dA}{dz} = -\beta_1 \frac{dA}{dt} - \frac{j}{2}\beta_2 \frac{d^2A}{dt^2} + \frac{1}{6}\beta_3 \frac{d^3A}{dt^3} - \frac{\alpha}{2}A + j\gamma\left(1 + \frac{j}{\omega_0}\frac{d}{dt}\right)\left(A(z,t)\int_0^\infty R(t')|A(z,t-t')|^2 dt'\right) \tag{2}$$

where the response function $R(t)$ includes the instantaneous electronic (Kerr) response and the vibrational (Raman) contributions. For shorter time scales, lower than 1 fs, the real part of the susceptibility is dominant and arises from the non-resonant virtual electronic transitions. This interaction is modelled by an instantaneous delta function. For longer time scales, over 100 fs, the imaginary contribution is dominant arising from the phonon lifetime. This part of the interaction is modelled by a single Lorentzian line centred on the optical phonon frequency [11]–[13]

$$R(t) = (1 - f_R)\delta(t) + f_R h_R(t) \tag{3}$$

where f_R represents the fractional contribution of the delayed Raman response, $\delta(t)$ is the Dirac delta function and $h_R(t)$ – the temporal variation of the Raman response function, given by [11]

$$h_R(t) = \frac{\tau_1^2 + \tau_2^2}{\tau_1 \tau_2^2} \exp\left(-\frac{t}{\tau_2}\right) \sin\left(\frac{t}{\tau_1}\right). \tag{4}$$

This function has a Lorentzian shape in the spectral domain.

The first adjustable parameter for the Raman response function τ_1 and the second adjustable parameter for the Raman response function τ_2 are related with the phonon frequency and bandwidth of the Lorentzian line, respectively. The Raman time constant can be obtained from the Raman delay response

$$T_R = \int_0^\infty tR(t)\mathrm{d}t. \tag{5}$$

3. Analysis of the stimulated Raman scattering

Under quasi-continuous conditions, the interaction between the pump and the Stokes wave along the propagation direction z is described by the following set of coupled differential equations [9]:

$$\frac{\mathrm{d}I_s}{\mathrm{d}t} = g_r I_s I_p - \alpha_s I_s, \tag{6}$$

$$\frac{\mathrm{d}I_p}{\mathrm{d}t} = -\frac{\omega_p}{\omega_p} g_r I_s I_p - \alpha_p I_p \tag{7}$$

where I_s is the Stokes intensity with a optical frequency ω_s, I_p – the pump intensity with optical frequency ω_p and g_r represents the material Raman gain coefficient, which scales inversely with the pump wavelength [14]. The absorption coefficients α_s and α_p account for the losses at the Stokes and pump frequencies, respectively.

Neglecting the pump depletion the Stokes intensity along propagation can be obtained from the previous coupled equations:

$$I_s(L) = I_s(0)\exp(g_r I_p(0)L_{\mathrm{eff}} - \alpha_s L) \tag{8}$$

where L_{eff} is the effective interaction length which replaces the real fibre length L in order to account for the exponential decay of the power along propagation. The effective length is given by

$$L_{\mathrm{eff}} = \frac{1}{\alpha_p}[1 - \exp(-\alpha_p L)]. \tag{9}$$

The use of Eq. (8) requires an input power signal ($I_s(0)$), but in practice the SRS is built from spontaneous Raman scattering occurring through the fibre length. This is

equivalent to the injection of one fictitious photon at the input [9]. The intensity of the signals can be converted to optical power, using the effective area of the fibre (A_{eff})

$$P = IA_{\text{eff}}. \tag{10}$$

Therefore the Raman gain coefficient in the fibre can be given by

$$g_r^{\text{fibre}} = \frac{g_r}{A_{\text{eff}}}. \tag{11}$$

The Raman threshold is defined as the input pump power at which the Stokes power becomes equal to the pump power at the fibre output. Considering a Lorentzian Raman gain spectrum with maximum gain value of $g_r^{\max}$, it can be approximated to

$$P_{\text{th}} \approx \frac{16 A_{\text{eff}}}{k_p L_{\text{eff}} g_r^{\max}} \tag{12}$$

where k_p is a polarization factor, which lies between 1, when the polarization of the Stokes and pump signal are parallel and preserved along propagation, and 1/2 when the polarizations are completely scrambled.

As mentioned before, the silica non-linear third-order susceptibility consists of an electronic part and a Raman part [15]

$$\chi^{(3)}(\omega) = \chi_E^{(3)} + \chi_R^{(3)}(\omega) \tag{13}$$

where $\chi_E^{(3)}$ is the electronic non-resonant real part, and $\chi_R^{(3)}(\omega)$ is the Raman resonant complex part. The real part of the susceptibility is responsible for the self-phase modulation and parametric non-linear effects. The imaginary part is responsible for the Raman effects and determines the Raman gain coefficient [16]

$$g_r(\Delta\omega) = \frac{4\pi\omega_0 k_p}{cn} \operatorname{Im}(\chi_R^{(3)}(\Delta\omega)) \tag{14}$$

where c is the speed of light, n – the linear refractive index, and $\operatorname{Im}(\chi_R^{(3)}(\Delta\omega))$ stands for the imaginary part of the argument. The Raman time constant is related to the slope of the Raman gain by [16]

$$T_R = \frac{2\pi k_p}{nn_2} \left[\frac{\mathrm{d}(\operatorname{Im}(\chi_R^{(3)}))}{\mathrm{d}(\Delta\omega)} \right]_{\Delta\omega = 0} \tag{15}$$

where n_2 is the non-linear refractive index. Therefore,

$$T_R = \frac{c}{n_2\omega_0 4\pi} \left[\frac{\mathrm{d}(g_R(\Delta f))}{\mathrm{d}(\Delta f)} \right]_{\Delta f = 0}. \tag{16}$$

The Raman gain coefficient can also be related to the Raman response function by [9]

$$g_R(\Delta\omega) = \frac{\omega_0}{cn} f_R k_p \chi^{(3)} \mathrm{Im}[\tilde{h}_R(\Delta\omega)] \tag{17}$$

where $\tilde{h}_R(\Delta\omega)$ is the Fourier transform of $h_R(t)$.

4. Measurement of the Raman gain

Several techniques have been used to measure the SRS, such as the measurement of the Raman self-frequency shift of a short optical pulse [16], measurement of the Raman induced power tilt in a DWDM transmission system [17]–[19] and the measurement of the Raman scattering power spectrum generated [20]. We calculate the Raman gain coefficient of a standard single mode optical fibre (SMF), measuring the optical power transferred from a shorter wavelength high intensity continuous wave optical signal to a longer wavelength counter-propagation broadband probe signal [21].

The experimental set-up is shown in Fig. 1. A broadband probe signal, shown in Fig. 2, provided by the amplified spontaneous emission (ASE) noise from the erbium doped fibre amplifier (EDFA) is injected at one fibre end (from now on, this signal will be treated as Stokes signal). At the other end a high intensity pump signal is injected at 1530 nm, in a counter propagation direction, through an optical circulator. The optical power of the broadband signal is measured in an optical spectrum analyser (OSA) with a 0.1 nm resolution and 100 acquisitions averaging. An optical isolator prevents the pump signal from entering the EDFA.

The set of coupled differential Eqs. (6) and (7) can be solved analytically when the frequencies of the two carriers are assumed to be equal and when the intensity of one of the two signals is much stronger than the other [21]. They must be changed to include

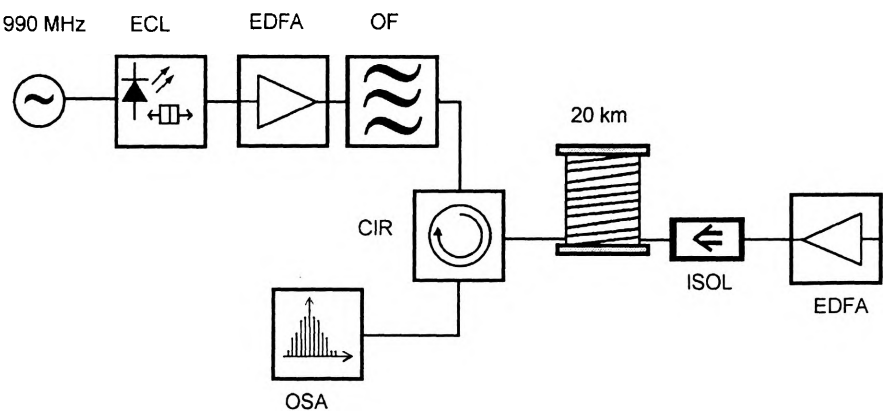

Fig. 1. Experimental set-up used to measure the Raman gain coefficient. ECL – external cavity laser, EDFA – erbium doped fibre amplifier, OF – optical filter, OSA – optical spectrum analyser, CIR – optical circulator, ISOL – optical isolator.

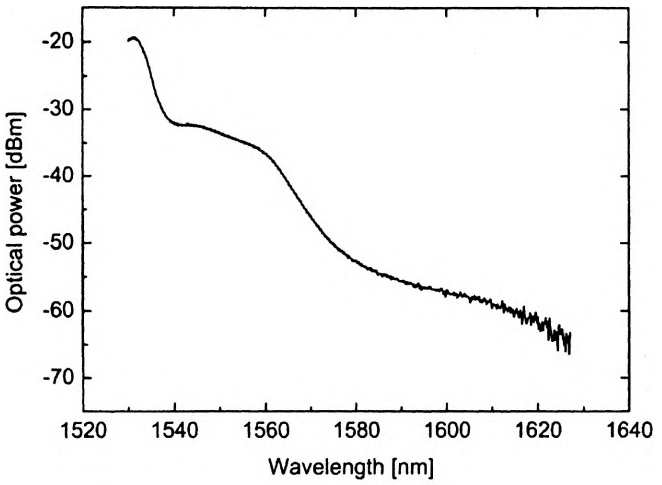

Fig. 2. ASE spectrum of the broadband source.

the polarization effect, through k_p. When the pump power is stronger than the Stokes signal, the power of the Stokes signal at the OSA input is given, from Eq. (8), by

$$P_{\text{Stokes}}(L) = P_{\text{Stokes}}^{\text{pump}=0}(L)\exp\left(g_r(\lambda)P_{\text{pump}}(0)\frac{L_{\text{eff}}}{A_{\text{eff}}}k_p\right) \tag{18}$$

where $P_{\text{Stokes}}(L)$ is the power of the Stokes signal at the fibre output, $P_{\text{Stokes}}^{\text{pump}=0}(L)$ – the power of the Stokes signal at the fibre output without the pumping signal and $P_{\text{pump}}(0)$ – the pumping power. The factor of 1/2 (value of k_p) appears, since the fibre is considered long enough to randomize completely the polarization of both the pump and the Stokes waves. Solving Eq. (18) for g_r

$$g_r(\lambda) = \frac{\ln\left(\dfrac{P_{\text{Stokes}}(L)}{P_{\text{Stokes}}^{\text{pump}=0}(L)}\right)A_{\text{eff}}}{0.5P_{\text{pump}}(0)L_{\text{eff}}}. \tag{19}$$

The difference in logarithmic units of the measured Stokes signal with and without pump signal is known as Raman gain and is given by

$$G_r(\lambda) = 10\log\left(\frac{P_{\text{Stokes}}(L)}{P_{\text{Stokes}}^{\text{pump}=0}(L)}\right) \tag{20}$$

which is related to the Raman coefficient by

$$G_r(\lambda) = 4.35\,\frac{1}{2}\,g_r(\lambda)P_{\text{pump}}(0)\frac{L_{\text{eff}}}{A_{\text{eff}}}. \tag{21}$$

The optical spectrum of the Stokes signal was measured between 1530 nm and 1620 nm for a peak pump power of 149.0 mW. The high intensity pump signal was obtained from an external cavity laser (ECL), modulated at 990 MHz in order to increase the Brillouin threshold beyond the working optical power. Following the ECL there is an EDFA for signal boosting and a 1.6 nm optical filter for ASE reduction. We use a 20 km optical fibre reel with a 0.206 dB/km or 0.0474 km^{-1} optical attenuation and an effective area of 91.61 μm^2, which results in an effective fibre length of 12922 m. The optical circulator and isolator used were designed for the *C* (center wavelength band, 1530–1570 nm) + *L* (long wavelength band, 1570–1610 nm) spectral band, however the spectral characteristics of these elements were taken into account in the determination of the Raman gain. The Raman gain is the difference observed in the Stokes signal with and without pump signal and is shown Fig. 3.

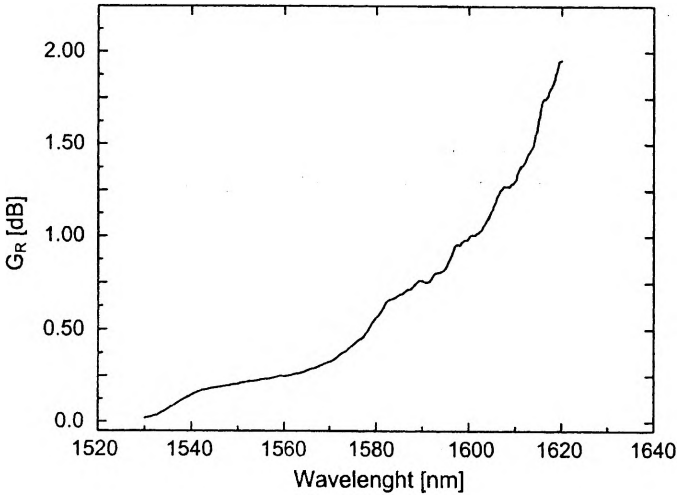

Fig. 3. Measured Raman gain.

Figure 4 displays the calculated Raman gain coefficient as a function of the Raman frequency shift to the pump wavelength, using expression (21). The result obtained is compared with values indicated in reference [22] for pure bulk silica pumped at 1550 nm.

The difference between these two curves is due to the polarization effect and to the presence of germanium used to increase the optical fibre core index, and it is recognised as being responsible for the change in profile of the Raman gain curve, reducing its bandwidth [23].

In Figure 5, there are shown the Raman gain coefficient, with the linear regression fit used to calculate the Raman gain coefficient slope and the Raman time constant through expression (16), resulting in the values of 7.48×10^{-27} $mW^{-1}Hz^{-1}$ and 3.03 fs,

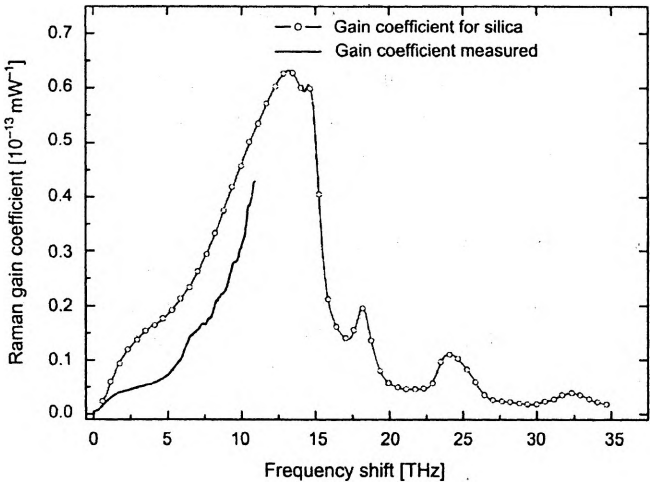

Fig. 4. Raman gain coefficient measured in the optical fibre and reported for bulk silica.

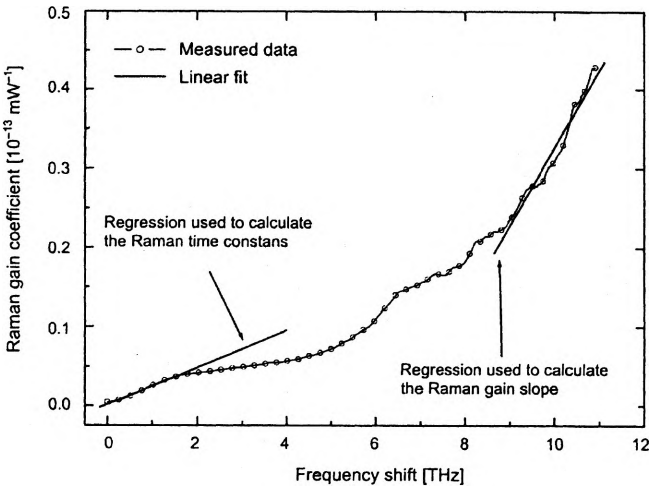

Fig. 5. Raman gain coefficient and linear fit to experimental data.

respectively. The Raman time constant calculation is based on the slope gain coefficient curve around the pump frequency (2.34×10^{-27} $mW^{-1}Hz^{-1}$). These values of the Raman gain slope and time constant are in agreement with previously reported data [16], [17]. The value of the Raman time constant is in good agreement with the value of 3.0 fs reported based on the Raman self-frequency shift [16]. The value of the Raman gain slope is 49.6% higher than the value reported in [17] for SMF, obtained by measuring the SRS induced spectral tilt, within a 3.125 THz window. It must be

emphasised that our value is the local slope over a 2 THz window which begins at 8 THz from the pump signal.

The value of the Raman time constant is sufficient to solve the propagation Eq. (1), but to solve expression (2) it is necessary to know the parameters τ_1, τ_2 and f_R, which can be obtained from the complete profile of the gain curve.

5. Spontaneous Raman scattering measurement

The Raman gain coefficient can be obtained by spontaneous Raman scattering spectroscopy measurements. The material Raman scattering coefficient is related to the zero Kelvin spontaneous Raman scattering cross-section through [23]

$$g_r(\Delta\upsilon) = \frac{\sigma_0(\Delta\upsilon)\lambda^3}{c^2 h n(\upsilon)^2}. \tag{22}$$

The cross-section collected data are measured at room temperature but these data can be reduced to the zero Kelvin cross-section σ_0 using:

$$\sigma_0(\Delta\upsilon) = \sigma_{300\mathrm{K}}(\Delta\upsilon)\left[1 + \frac{1}{\exp\left(\frac{h\Delta\upsilon}{k_B T}\right) - 1}\right]^{-1} \tag{23}$$

where h is the Planck constant, k_B the Boltzmann and T is the absolute temperature. We measured the spontaneous Raman scattering of a standard single mode optical fibre. The fibre was stripped and cleaned in such a way as to expose the cladding. In the measurement the 488 nm line of an argon ion laser is used as exciting source, pumping the fibre in a radial direction, helped by a microscope with a 100 X objective. This allows us to calculate the scattering cross-section in an approximate way, since we do not perform a calibration against a known standard and due to the geometry of the sample.

Using Eqs. (22) and (23) the Raman gain coefficient curve is obtained. Since such data are measured with a pump signal of 488 nm and the gain coefficient scales inversely with pump wavelength, the results must be scaled for the effect of wavelength in order to be compared with the results measured with a 1530 nm pump signal. The polarization averaging effect should also be included. Therefore the results should be multiplied by the scaling factor $(1/2 \cdot 488/1530)$, which results in the data shown in Fig. 6.

From this spectrum the value for the centre f_c and the full width at half maximum value Δf can be obtained, being 12.841 THz and 5.521 THz, respectively. This can be used to calculate the Raman adjustable parameters by:

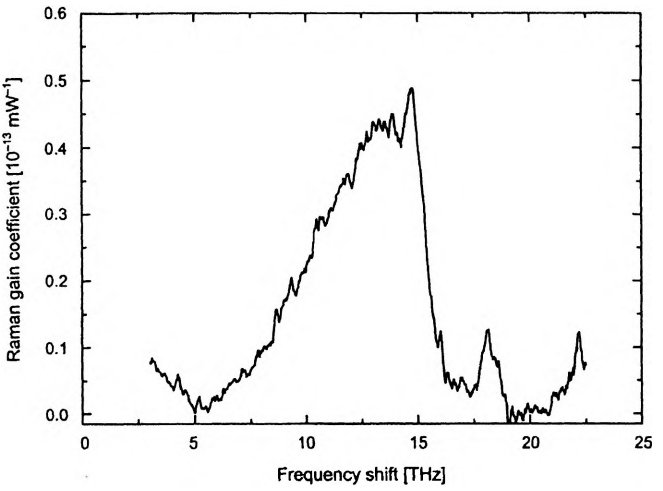

Fig. 6. Raman gain coefficient.

$$\tau_1 = \frac{1}{2\pi f_c}, \tag{24}$$

$$\tau_2 \approx \frac{1}{\sqrt{2}\pi\Delta f}, \tag{25}$$

leading to 12.340 fs and 40.78 fs for τ_1 and τ_2, respectively. In paper [9] these parameters are given the values of 12 fs and 32.2 fs, respectively. The value of τ_1 obtained by us differs from that obtained by a 3.3% difference, which is not significant for simulation purposes. On the other hand, the value of τ_2 is significantly different. Whereas the value given in [9] was obtained for pure bulk silica, our value was obtained directly from an optical fibre with a Ge doped core that is known to substantially deform the Raman gain coefficient spectrum.

The peak value of the Raman gain coefficient ($g_r^{\max}$), obtained at f_c, can be extrapolated with precision from the slope of the Raman curve previously obtained, which results in a value of 0.540×10^{-13} mW^{-1}. This value is also comparable with published results [20]. Using Eq. (17) the value of f_R could be estimated at 0.160 which is comparable with the value of 0.18 reported in [9].

6. Simulation

The previously obtained values are used as the simulation parameters. Figure 7 shows the temporal Raman response function obtained using Eq. (4).

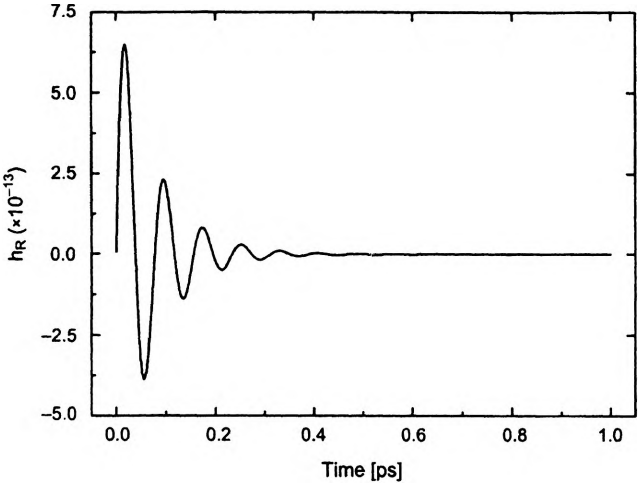

Fig. 7. Temporal variation of the Raman response function.

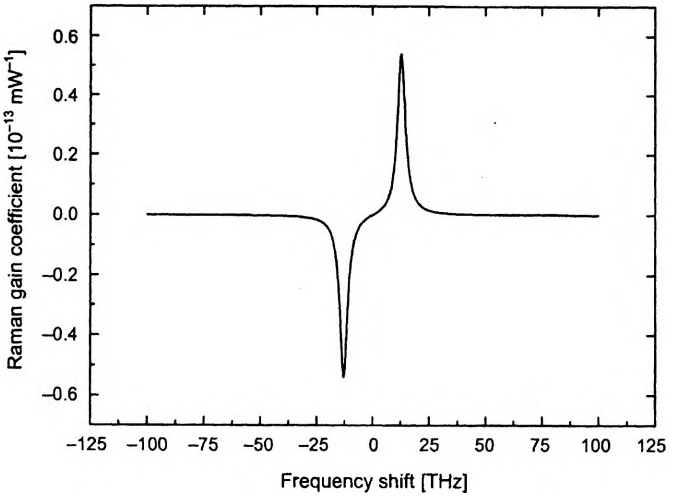

Fig. 8. Raman coefficient numerically calculated from the spectral variation of the Raman response function.

The imaginary part of the Fourier transform Raman response function can be used through Eq. (17) to calculate the Raman coefficient, displayed in Fig. 8.

The experimental set-up described in Sec. 4 is also modelled in a commercial photonic simulator, VPI Transmission Maker© from Virtual Photonics [24]. All the experimental parameters are mapped to the simulation scenery. The following values are also used for the fibre dispersion: $\beta_2 = -21.44$ ps^2/km and $\beta_3 = 0.151$ ps^3/km. The

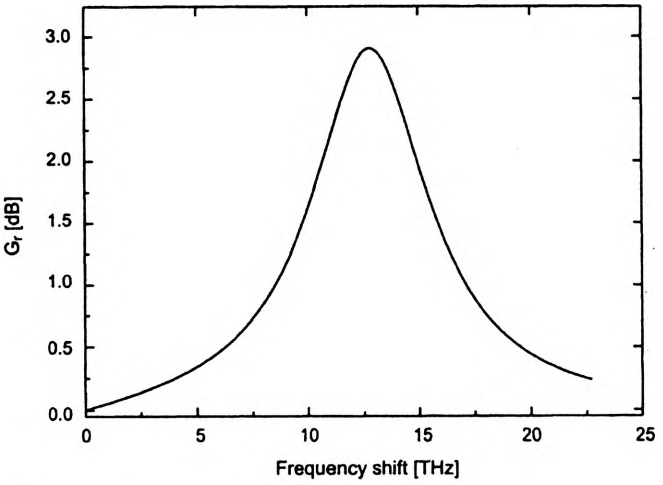

Fig. 9. Simulated Raman gain.

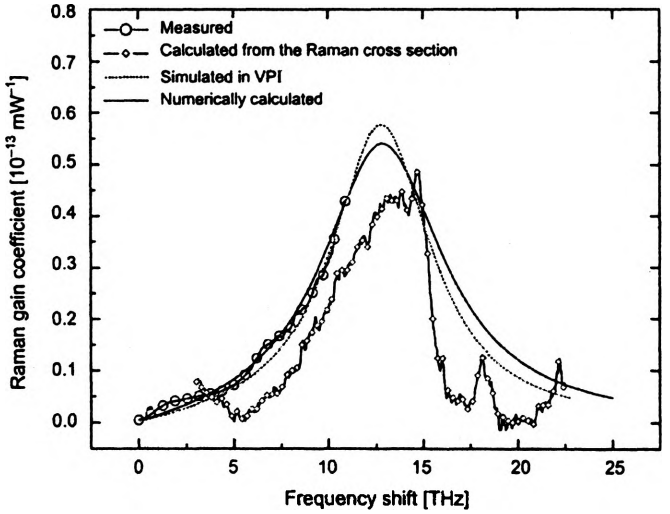

Fig. 10. Comparison of Raman coefficient curves, measured and simulated.

curve for the Raman gain given in Fig. 9 is comparable with the experimental results of Fig. 3.

Figure 10 displays the comparison of the Raman gain coefficients experimentally measured, calculated from the Raman cross-sections, numerically simulated and simulated in the commercial simulator.

As can be seen the calculated parameter can be used in simulation, yielding a good agreement with the experimental results.

7. Conclusions

A method of measuring the Raman gain coefficient based on the power transfer between a high intensity pump and a counter propagation broadband probe signal has been developed. The results have been complemented with spontaneous Raman scattering spectroscopy data.

From these measurements, the Raman effect has been fully characterized and the values for the Raman gain slope, maximum value of the gain coefficient, the Raman time constant, first and second parameters of the Raman response function and fractional contribution of the delayed Raman response, have been obtained. These values are in agreement with previous reports and consistent with the simulation results obtained.

The Raman gain coefficient versus frequency shift spectrum appears to be similar in shape as the published results, with smaller differences of absolute values. The difference can be due to a different phonon distribution in fibres, as non crystalline nature differs from the best ordered bulk silica.

Using the measured fibre Raman characterized we are able to estimate by simulation the impact of the Raman effect on long haul optical communications systems.

Acknowledgment – The work was financed by the Portuguese scientific program FCT-PRAXIS XXI (PRAXIS XXI/BD/17227/98) through the DAWN and WIDCOM(POSI/35574/99/CPS/2000) projects and by Portugal Telecom Inovação through the ANDES project (P152). This work also received financial support from CAPES, CNPq, PRONEX (Brazilian Agencies) and ICCTI, being part of the activities of the CAPES/ICCTI project 58/00.

References

[1] RAMAN C.V., KRISHNAN K.S., Nature **121** (1928), 501.
[2] BARNARD C.W., MYSLINSKI P., PAN X., CHROSTOWSKI J., J. Lightwave Technol. **13** (1995), 115.
[3] CHRAPLYVY A.R., HENRY P.S., Electron. Lett. **19** (1983), 641.
[4] MAZURCZY V.J., SHAULOV G., GOLOVCHENCKO E.A., IEEE Photon Technol. Lett. **12** (2000), 1573.
[5] CHRAPLYVY A.R., Electron. Lett. **2** (1984), 58.
[6] TARIQ S., PALAIS J.C., Fiber Integr. Opt. **15** (1996), 335.
[7] GRANDPIERRE A.G., CHRISTODOULIDES D.N., SCHIESSER W.E., MCINSTOSH C.M., TOULOUSE J., Opt. Commun. **194** (2001), 319.
[8] GORDON J.P., Opt. Lett. **11** (1986), 662.
[9] AGRAWAL G.P., *Nonlinear Fiber Optics*, Academic Press, 2nd edition, London 1995.
[10] MAMYSHEV P.V., CHERNIKOV S.V., Opt. Lett. **15** (1990), 1076.
[11] BLOW K.J., WOOD D., IEEE J. Quantum Electron. **25** (1989), 2665.
[12] CHERNIKOV S.V., MAMYSHEV P.V., J. Opt. Soc. Am. B **8** (1991), 1633.
[13] STOLEN R.H., GORDON J.P., TOMLINSON W.J., HAUS H.A., J. Opt. Soc. Am. B **6** (1989), 1159.
[14] CHRAPLYVY A., J. Lightwave Technol. **8** (1990), 1548.
[15] GOLOVCHENKO E.A., MAMYSHEV P.V., PILIPETSKII A.N., DIANOV E.M., J. Opt. Soc. Am. B **8** (1991), 1626.

[16] ATIEH A.K., MYSLINSKI P., CHROSTOWSKI J., GALKO P., J. Lightwave Technol. **17** (1999), 216.
[17] BIGO S., GAUCHARD S., BERTAINA A., HAMAIDE J.P., IEEE Photon Technol. Lett. **11** (1999), 671.
[18] ZIRNGBL M., Electron. Lett. **34** (1998), 789.
[19] SHAULOV G., MAZURCZYK V.J., GOLOVCHENKO E.A., *Measurement of Raman gain coefficient for small wavelength shifts*, [In] Proc. OFC2000, TuA4-1, 2000, pp. 12–14.
[20] MAHGEREFTEH D., BUTLER D.L., GOLDHAR J., ROSENBERG B., BURDGE G.L., Opt. Lett. **21** (1996), 2026.
[21] SUBIAS J., PELAYO J., HERAS C., BLASCO P., ALONSO R., Opt. Commun. **176** (2000), 387.
[22] MCINTOSH C.M., GRANDPIERRE A.G., CHRISTODOULIDES D.N., TOULOSE J., DELAVAUX J.M.P., IEEE Photon Technol. Lett. **13** (2001), 302.
[23] WILLIAMS D.L., *The design of novel Silica based fibre devices for telecommunications*, Ph.D. Thesis, Sheffield University, 1993.
[24] LOWERY A., LENZMANN O., KOLTCHANOV I., MOOSBURGER R., FREUND R., RICHTER A., GEORGI S., BREUER D., HAMSTER H., IEEE J. Selected Topics Quantum Electron. **6** (2000), 282.

Received January 31, 2003
in revised form March 19, 2003